



biblio.ugent.be

The UGent Institutional Repository is the electronic archiving and dissemination platform for all UGent research publications. Ghent University has implemented a mandate stipulating that all academic publications of UGent researchers should be deposited and archived in this repository. Except for items where current copyright restrictions apply, these papers are available in Open Access.

This item is the archived peer-reviewed author-version of: The impact of the injection mold temperature upon polymer crystallization and resulting drug release from immediate and sustained release tablets

Authors: Van Renterghem J., Dhondt H., Verstraete G., De Bruyne M., Vervaet C., De Beer T.

In: International Journal of Pharmaceutics, 541(1-2), 108-116

To refer to or to cite this work, please use the citation to the published version:

Van Renterghem J., Dhondt H., Verstraete G., De Bruyne M., Vervaet C., De Beer T. (2018)
The impact of the injection mold temperature upon polymer crystallization and resulting drug release from immediate and sustained release tablets

International Journal of Pharmaceutics 541(1-2): 108-116

DOI: 10.1016/j.ijpharm.2018.01.053

1 **The impact of the injection mold temperature upon polymer crystallization and resulting drug**
2 **release from immediate and sustained release tablets.**

3 Jeroen Van Renterghem¹, Heleen Dhondt¹, Glenn Verstraete², Michiel De Bruyne³, Chris Vervaet²,
4 Thomas De Beer¹

5

6 ¹ Laboratory of pharmaceutical process analytical technology, Ottergemsesteenweg 460, 9000,
7 Ghent, Belgium

8 ² Laboratory of pharmaceutical technology, Ottergemsesteenweg 460, 9000, Ghent, Belgium

9 ³ Inflammation Research Center, VIB, Ghent, Belgium and Department of Biomedical Molecular
10 Biology, Ghent University, 9052 Ghent, Belgium.

11 ³ Department of Plant Systems Biology, VIB, Ghent, Belgium and Department of Plant Biotechnology
12 and Bioinformatics, Ghent University, 9052 Gent, Belgium.

13

14

15

16

17 *Corresponding author: Jeroen Van Renterghem

18 Laboratory of Process Analytical Technology, Ghent University, Ottergemsesteenweg 460, 9000 Ghent,
19 Belgium

20 TEL: 0032 9 264 8039

21 FAX: 0032 9 264

22 E-MAIL: jeroen.vanrenterghem@ugent.be

23

24

25 Abstract

26 It was the aim of this study to elucidate the impact of the injection mold temperature upon the
27 polymer crystallinity, its microstructure and the resulting drug release from immediate and sustained
28 release tablets containing semi-crystalline polymers. The immediate release formulation contained
29 20% (w/w) ketoprofen (KETO) in poly (ethylene oxide) (PEO) and the sustained release formulation
30 contained 20 - 40% (w/w) metoprolol tartrate (MPT) in polycaprolactone (PCL). Physical mixtures of
31 drug-polymer were characterized via isothermal crystallization experiments using DSC and rheological
32 measurements to elucidate the impact of the drug solid-state upon the crystallization kinetics. Tablets
33 were prepared using various thermal histories (extrusion barrel temperature and injection mold
34 temperatures). Polymer crystallinity and microstructure in the tablets was characterized via DSC and
35 polarized optical microscopy. The polymer microstructure was altered by the various applied thermal
36 histories. The differences in PEO crystallinity induced by the various mold temperatures did not affect
37 the KETO dissolution from the tablets. On the other hand, MPT (20 - 40% w/w) dissolution from the
38 PCL matrix when extruded at 80 °C and injection molded at 25 and 35 °C was significantly different due
39 to the changes in the polymer microstructure. More perfect polymer crystals are obtained with higher
40 mold temperatures, decreasing the drug diffusion rate through the PCL matrix. The results presented
41 in this study imply that the injection mold temperature should be carefully controlled for sustained
42 release formulations containing hydrophobic semi-crystalline polymers.

43

44

45

46 Keywords: Solid dispersion, injection molding, semi-crystalline polymers, rheology, crystallization

47 **Abbreviations**

48	API	Active Pharmaceutical ingredient
49	DSC	Differential scanning calorimetry
50	HME	Hot Melt Extrusion
51	KETO	Ketoprofen
52	MPT	Metoprolol tartrate
53	NSAID	Nonsteroidal anti-inflammatory drug
54	PCL	Polycaprolactone
55	PEO	Poly (Ethylene Oxide)
56	POM	Polarized optical microscopy
57	T_c	Isothermal crystallization temperature
58	T_m	Melt temperature
59	T_m°	Equilibrium melting temperature
60		
61		
62		
63		
64		
65		
66	1	Introduction

67 The well-established melt processing technique hot-melt extrusion (HME) can be combined with
68 injection molding (IM) for downstream processing. Herewith, the extrusion step is conducted to melt
69 the raw materials (i.e., drug + polymer) using elevated barrel temperatures and shearing forces from
70 the rotating screw(s), to obtain a homogeneous melt at the end of the die. In a continuous manner,
71 subsequent injection of the melt into a mold cavity yields the final dosage form. In combination, a lot
72 of opportunities for the pharmaceutical industry exist towards production of immediate and sustained
73 release solid dosage forms, depending on the type of polymer used. Another strength of the HME/IM
74 combination is the large variety of drug products that can be produced: matrix tablets (Bruce et al.,
75 2005), implants (Rothen-Weinhold et al., 1999), transdermal drug delivery systems (Crowley et al.,
76 2004; Prodduturi et al., 2005), vaginal rings (Clark et al., 2012).

77 When using HME in combination with IM, characterization of the drug-polymer melt formulation
78 by rheological measurements is essential to predict the processability. An indicative range of the
79 processing temperature can be established by a rheological characterization of the flow properties of
80 the molten dispersions (Gupta et al., 2012; Parikh et al., 2014; Van Renterghem et al., 2017; Verstraete
81 et al., 2016). When using semi-crystalline polymers as carrier during HME and IM, these polymers are
82 processed above their melting temperature to decrease their melt viscosity sufficiently to allow a
83 steady flow of the polymer through the extruder barrel and into the mold. Upon cooling from the melt,
84 semi-crystalline polymers solidify when nuclei are formed and crystallization commences. Depending
85 on the cooling rate (i.e., mold temperature) and the solid-state of the drug content, the crystallization
86 rate of the polymer is altered as well as the polymer's crystalline microstructure and crystallinity
87 percentage. Jeong et al. has shown that a small difference in the polymer morphology can influence
88 the drug release from microspheres prepared via solvent evaporation (Jeong et al., 2003). Annealing
89 the PCL microspheres at 25, 40 and 50 °C yielded differences in the drug release. As the size of the
90 lamellae was larger for the annealed sample at 50 °C compared to the 25 °C sample, the drug diffusion
91 was affected. Other researchers also demonstrated that the polymer crystallinity had a significant
92 impact on the drug release from other semi-crystalline polymer systems prepared via solvent

93 evaporation (Alexis, 2005; Karavelidis et al., 2011; Zilberman, 2005). However, to the best of our
94 knowledge, this thermal history effect upon drug release was not investigated for injection molded
95 matrix systems.

96 It was the aim of this study to investigate the influence of various processing conditions (i.e.,
97 extrusion barrel temperature and injection mold temperature) upon the drug release from both
98 immediate and sustained release drug formulations prepared by HME and IM. Physical mixtures of
99 drug and semi-crystalline polymer were first characterized by DSC and rheological experiments to
100 obtain knowledge about their processability and the influence of the drug solid-state upon polymer
101 crystallization. Injection-moulded tablets were prepared using various extrusion barrel temperatures
102 and injection mold temperatures. These tablets were analyzed using DSC to determine the polymer
103 crystallinity and the drug solid-state. Polarized optical microscopy (POM) was used to investigate the
104 polymer microstructure of sustained release tablets containing PCL as matrix. Dissolution tests were
105 performed to investigate the impact of mold temperature (i.e. thermal history) on the resulting drug
106 release.

107 2 Experimental

108 2.1 Materials

109 The immediate release formulation contained 20% (w/w) ketoprofen (KETO) in poly (ethylene
110 oxide) (PEO). KETO (SIMS, Florence, Italy) is a non-steroidal anti-inflammatory drug (NSAID) with poor
111 water solubility (BCS class-II), ideal as model drug for the preparation of immediate release
112 formulations. KETO has a melting point of 94 °C (Sweetman, 2009). PEO (POLYOX™ WSR N10 LEO NF,
113 Dow Chemical Company, Michigan, USA) is a water soluble semi-crystalline polymer with a glass
114 transition temperature of -67 °C and a melting point of 65 °C. The average molecular weight is 100,000
115 g/mol (Suwardie et al., 2011). The enthalpy of fusion for 100% crystalline PEO is 205 J/g (Zhao et al.,
116 2005). KETO/PEO interactions can be detected even in non-melt-processed blends at temperatures as
117 low as 43 °C (Schachter et al., 2004). Because of these strong interactions, KETO is dissolved in the PEO
118 matrix during the isothermal crystallization (section 2.2.1) and extrusion/injection molding
119 experiments (section 2.2.2).

120 The sustained release formulation contained 20 and 40% (w/w) metoprolol tartrate (MPT) in PCL.
121 MPT (Utag, Amsterdam, The Netherlands) is a cardio-selective beta blocker belonging to the BCS Class-
122 I drugs and is thus an interesting model drug to prepare extended release formulations. MPT crystals
123 have a melting point of approximately 123 °C (Sweetman, 2009). PCL (Capa™ 6506, Perstorp, Malmö,
124 Sweden) is a biodegradable, semi-crystalline and hydrophobic polyester that is poorly water soluble
125 and is used to obtain a controlled release of the API (Active pharmaceutical ingredient). The drug
126 release from this polymer is via diffusion and biodegradation of the polymer is slow (Jeong et al., 2003;
127 Kamaly et al., 2016). PCL has a melting point of approximately 60 °C, a glass transition temperature of
128 -60 °C and an average molecular weight of 50,000 g/mol. The heat of fusion for the 100% crystalline
129 polymer is 139.5 J/g (Gupta et al., 2012).

130

131

132 2.2 Methods

133 2.2.1 Characterization of raw materials and physical mixtures

134 *Differential scanning calorimetry*

135 A DSC Q2000 (TA instruments, New Castle, USA) was used to perform all thermal analysis of the
136 raw materials, the physical mixtures and the IM tablets. All experiments were performed using Tzero
137 pans containing approximately 3 mg of sample. Indium was used to calibrate the instrument. Heat-
138 cool-heat experiments were performed as followed: the sample was first equilibrated for 3 min at -70
139 °C, followed by a heating run at 10 °C/min to 140 °C which is above the drug melting points of KETO
140 and MPT. Also a heating run to a temperature below the melting point of MPT (i.e., 100°C) was
141 performed to study the crystallization of PCL upon cooling when MPT was still in its crystalline state.
142 The second cycle is a cooling run to -70 °C at 10 °C/min during which crystallization of the polymer can
143 be observed. The last cycle is a second heating at the same heating rate and temperature limits as the
144 first heating. All heat-cool-heat experiments were performed in triplicate.

145 Furthermore, isothermal crystallization experiments were conducted to study the crystallization
146 speed of the polymer at different isothermal temperatures. The experiments were performed as
147 followed: the physical mixture was first equilibrated for 3 min at a temperature above the polymer
148 melting point (see table 1). The sample was then quickly cooled (at 50 °C/min) to the isothermal
149 crystallization temperature and kept isothermal for one hour during which the sample crystallized. The
150 crystallized sample was again heated at 10 °C/min to determine the polymer melting point. The
151 samples containing MPT were equilibrated below (i.e., 80 °C for 20 and 40% (w/w) MPT) and above
152 (i.e., 140 °C for 20% (w/w) MPT) the drug melting temperature to determine the influence of the drug
153 solid-state upon the polymer crystallization speed.

154

155

156 *Rheology*

157 A Haake™ MARS™ III rheometer (Thermo Fisher, Waltham, USA) equipped with a 20 mm parallel
158 plate configuration was used for all rheological experiments. The lower stationary plate can be heated,
159 allowing to impose different thermal treatments on the sample. Physical mixtures were loaded onto
160 the bottom plate and were allowed sufficient time to soften and equilibrate before commencing the
161 tests. Temperature sweep experiments were performed using a heating/cooling rate of 2 °C/min at a
162 constant frequency (1Hz) and deformation (for PEO, PEO-20KETO, PCL = 2% and for PCL-20MPT
163 =0.01%) that was within the linear viscoelastic range. The sample was heated above the drug melting
164 temperature (i.e., 100 °C or 150 °C for -KETO and MPT formulations, respectively) and was then cooled
165 until crystallization was complete, at which point the sample was again reheated at 2 °C/min to above
166 the drug melting point.

167 Isothermal crystallization experiments can also be performed using a rheometer. First, the sample
168 is heated until the polymer is molten (PEO systems: 100 °C; PCL systems: 80 °C, 100 °C or 140 °C). Then
169 the sample is cooled down to the isothermal crystallization temperature (T_c) (shown in table 1) with a
170 cooling rate of 5 °C/min followed by a time sweep at T_c . The temperature, the frequency (1 Hz) and
171 the deformation (2%) are kept constant and the complex viscosity, loss and storage moduli are
172 determined as a function of time. Upon crystallization, the complex viscosity and moduli strongly
173 increase. The experiment is stopped once a plateau of the viscoelastic properties (G' and G'') is reached
174 or when the rheometer torque reached its maximum.

175 *Data analysis*

176 The experimental data obtained from the isothermal crystallization experiments was fitted by the
177 commonly used Avrami equation (Eq. 1) (Lorenzo et al., 2007; Piorkowska et al., 2006; Schick, 2009).

$$178 \quad 1 - V_c(t) = \exp(-kt^n) \quad (1)$$

179 Where V_c is the relative volumetric transformed fraction, n the Avrami index, k (min^{-n}) the
180 overall crystallization rate constant and t (min) is time. Crystallization starts with the formation of
181 nuclei, followed by a linear growth of these nuclei. In the Avrami fit, some parameters (i.e. n and k)
182 quantifying this nucleation and growth are introduced. For the data measured by DSC, an automated
183 tool developed by Lorenzo et al. was used to calculate the Avrami parameters (Lorenzo et al., 2007).
184 The Avrami fit was performed manually for the data (i.e., G' as function of time) obtained by rheological
185 measurements. For both DSC and rheological measurements, a linear range (representing 20 - 40%
186 transformed fraction, with $R^2 > 0.99$) was selected from the linearized Avrami equation (Eq. 2) to
187 calculate the Avrami parameters (i.e., n and k). In this region, n and k are calculated by the respective
188 slope and intercept.

$$189 \quad \text{Log} \left(\ln \frac{1}{1-V_c(t)} \right) = \text{Log}(k) + n\text{Log}(t) \quad (2)$$

190 The experimental half crystallization time ($t_{1/2}$) can also be obtained by fitting the Avrami equation
191 (Eq. 3). It should be noted that the absolute zero time (t_0) is determined as the time when the
192 isothermal crystallization temperature is reached.

$$193 \quad t_{1/2} = \left(\frac{\ln(2)}{k} \right)^{1/n} \quad (3)$$

194

195

196 2.2.2 Production of injection molded tablets

197 The Haake™ minilab co-rotating twin-screw extruder (Thermo Fisher, Waltham, USA) was used to
198 extrude the physical mixtures which were prepared with a mortar and pestle. The extruder was used
199 in continuous mode (i.e. the recirculation channel was not used). The Haake™ MiniJet Pro Piston
200 (Thermo Fisher, Waltham, USA) injection molding system was used to prepare the IM tablets
201 (approximately 350 mg, h = 5 mm, d = 10 mm). The molten extrudate is directly inserted from the
202 extruder into the injector by holding the injector against the die of the extruder. The injector's
203 temperature is set to the same temperature as the extrusion barrel temperature to maintain the
204 thermal history and to prevent crystallization of the polymer before injection into the mold. After
205 proper filling of the injector, the molten mixture was injected into the mold with a pressure of 800 bar
206 during 5 s after which the pressure is kept constant for another 5 s at 500 bar to avoid expansion by
207 relaxation of the polymer. Annealing of the tablets is done in the mold at various set temperatures (25
208 and 35 °C) to apply different thermal histories upon the tablets during solidification. The mold
209 temperatures were selected based on the results of the rheological temperature sweep experiments
210 which are described in section 3.1.2. The tablets were kept in the mold for a certain time to allow
211 complete solidification and were then ejected by opening the mold. The various process parameters
212 used for HME and IM are shown in table 2. The 40% MPT physical mixture was only extruded at 80 °C
213 because higher temperatures (i.e., 140 °C) resulted in a too low viscous melt, which cannot be
214 extrudate or injection molded. The residence time in the extruder was approximately 100 s, defined
215 as the lag time from the feeder to the die and was measured by using a color tracer (cochineal red).

216

217

218

219

220 2.2.3 Tablet characterization

221

222 *Differential scanning calorimetry*

223 The IM tablets were analyzed by DSC using the same heating rate and limits as used for the physical
224 mixtures. Two samples were cut with a surgical blade from the edges of the flat-faced radius edged
225 tablets (3 tablets per thermal history setting). The first heating cycle of the IM tablets allows to
226 determine the drug and polymer's melting temperature (i.e., peak temperature T_m), the presence of
227 undissolved API particles and the calculation of the degree of crystallinity using Eq. 4 after processing
228 at various thermal histories (i.e., barrel temperature and mold temperature).

$$229 \quad X_c = \frac{\Delta H_f}{f \times \Delta H_{f100\%}} \times 100\% \quad (4)$$

230 where X_c (%) is the degree of crystallinity, ΔH_f (J/g) is the enthalpy of melting, f is the fraction
231 of drug or polymer and $\Delta H_{f100\%}$ is the enthalpy of melting for a fully crystalline polymer or drug.

232

233 *Polarized optical microscopy*

234 The crystalline microstructure of the sustained release tablets (i.e., PCL and PCL-20MPT extruded
235 at 80 °C) was visualized using a polarized optical microscope (Leica DM 2500P) equipped with a black
236 and white camera (Leica DFC360 FX). Samples were made by cutting the tablets in half (injection
237 direction) with a razor blade, trimmed and mounted on aluminum pin (see Fig. S11). Semi thin sections
238 of 3 μ m were obtained by cryosectioning at -40 °C using a Leica UC7 microtome equipped with a Leica
239 EM FC7 cyro chamber. Sectioning was performed in direction of the injection flow, from the center
240 towards to the outer edge of the tablet. To stretch the sample slices, they were placed in a drop of
241 glycerol on a glass slide and were then covered with a coverslip. Sections of PCL-20MPT were

242 immediately collected on a glass slide in the cryo-chamber. Curled sections were stretched manually
243 with an eyelash. The crystalline microstructure was analyzed semi-quantitatively using ImageJ
244 software (National Institutes of Health, Bethesda, MD) (Supplementary material Fig. SI2).

245 *Drug dissolution tests*

246 Immediately after processing, tablets (n = 5) from each thermal history setting were subjected to
247 *in vitro* dissolution testing. All formulations were tested using the same phosphate buffer solution (pH
248 = 6.6). A VK 7010 dissolution system with a VK 8000 automatic sampling station (Vankel Industries,
249 Edison, USA) was used. The vessels contained 900 mL of phosphate buffer solution (pH 6.6). The paddle
250 speed and the water bath temperature were kept constant at 100 rpm and $37 \pm 0,5$ °C, respectively.
251 Samples of 5 mL were withdrawn from the dissolution medium at predetermined time points (5, 10,
252 15, 30, 45, 60, 75, 90, 120 and 240 min for immediate release and 0.5, 1, 2, 4, 6, 8, 12, 16, 20 and 24
253 hours for sustained release formulations) and spectrophotometrically (Shimadzu 1650PC, Kyoto,
254 Japan) analyzed at a wavelength of 260 and 274 nm for KETO and MPT, respectively. Drug release
255 profiles were compared using the difference (f_1) and similarity factor (f_2) (as introduced by Moore and
256 Planner). (Moore and Planner, 1996). The drug release profiles show similarity when the value of f_2 is
257 greater than 50 and the value of f_1 is less than 15.

258

259 **3 Results & Discussion**

260 **3.1 Characterization of raw materials and physical mixtures**

261 **3.1.1 Crystallization kinetics**

262

263 The half crystallization times as function of the various applied isothermal crystallization
264 temperatures for the samples containing PEO are shown in Fig. 1c. The results clearly show that the

265 crystallization speed of PEO is slower with increasing isothermal crystallization temperatures. Earlier
266 research has demonstrated that a higher degree of undercooling (i.e., $\Delta T = T_m^\circ - T_c$, difference between
267 the equilibrium melting point and the isothermal crystallization temperature) results in a larger driving
268 force and speeds up crystallization (Crist and Schultz, 2016). The equilibrium melting temperature (T_m°)
269 is defined as the melting temperature of an extended chain crystal and is usually determined by the
270 Hoffman-Weeks approach. Therefore, the polymer is crystallized at various isothermal temperatures
271 (T_c) and subsequently reheated to determine the peak melting point. A linear fit is applied to the T_m vs
272 T_c data and the intercept of the fit with a line $T_c = T_m$ gives T_m° . Figure 1d shows that T_m° for the PEO-
273 20KETO (70.41 °C) sample is lower than for the neat polymer (72.61 °C). Consequently, the degree of
274 undercooling is also reduced at a given T_c , and nucleation and growth are much slower for PEO-20KETO
275 due to the lower degree of undercooling at the same T_c (Fowler et al., 2010). KETO is dissolved in the
276 molten polymer and inhibits chain folding by interacting with the polymer chains, inhibiting the
277 formation and folding of the polymer into lamellae (Marentette and Brown, 1998). For example, the
278 half crystallization time of pure PEO measured by rheology was 3.7 min at 47 °C, whereas it was almost
279 a tenfold (33.5 min) for PEO-20KETO. It should be noted that crystallization of PEO was not fully
280 completed within the experimental time (60 min) at 46 °C for the PEO-20KETO sample measured by
281 DSC (Fig. 1b), therefore the half crystallization calculation was not possible. Furthermore, the
282 rheological half crystallization times were always longer compared to the DSC experiments ($T_c = 46$ °C
283 not included). This can be explained by the differences in sample mass, the cooling rate differences (5
284 °C or 50 °C/min) and the sensitivity of the technique for detecting early crystallization. Moreover, these
285 results confirm that the frequency (1Hz) and deformation (2%) used during the rheological tests did
286 not affect the crystallization kinetics as otherwise the rheological measurements should have shown
287 faster crystallization compared to the DSC experiments due to the applied oscillatory stress.

288

289 Figure 2 shows the results of the isothermal crystallization experiments for the samples containing
290 PCL. Similar to the PEO results, PCL crystallization speed is also reduced at higher isothermal
291 temperatures. Both DSC and rheological crystallization experiments are complementary and showed
292 the same trend (Fig. 2 a - b). Both techniques indicated that the solid-state of the drug in the polymer
293 melt had an impact upon the crystallization speed of PCL. The crystallization speed of PCL was
294 depressed when the PCL-MPT mixture was heated above the melting temperature of MPT and
295 subsequently cooled to the isothermal crystallization temperature. Molten MPT clearly acted as a
296 plasticizer and inhibited PCL crystallization. For example, the half crystallization time measured by DSC
297 was 10.13 min for pure PCL at 43 °C and 21.30 min for the plasticized PCL melt. At 44 °C, crystallization
298 was not completed within the experimental time (60 min) during the DSC run as can be seen in Fig. 2d.
299 In contrast to molten MPT, crystalline MPT increased the crystallization speed of PCL. Crystalline MPT
300 acted as nucleating agent, decreasing the half crystallization time from 10.13 min for PCL to 9.39 min
301 for PCL-20MPT and 9.41 min for PCL-40MPT at 43 °C. Similar results are determined from the
302 rheological measurements (Fig. 2b), supporting the hypothesis. Increasing the MPT concentration from
303 20 to 40% did not result in a further increase of the polymer crystallization speed, suggesting that the
304 nucleating efficiency of crystalline MPT reached a saturation point. This finding is supported by the
305 equilibrium melting temperature, which slightly increased by the addition of crystalline MPT (T_m° PCL
306 = 61.46 °C T_m° PCL-20MPT = 62.36 °C ; T_m° PCL-40MPT = 61.82 °C). Therefore, the driving force for
307 nucleation and crystal growth of PCL increased by the addition of MPT crystals. Furthermore, the half
308 crystallization times measured by rheology were longer than the half crystallization times measured
309 by DSC, as was also the case for the PEO samples.

310

311

312 3.1.2 Rheological characterization

313 Figure 3 shows the complex viscosity as function of temperature for samples containing PEO (Fig.
314 3a) and PCL (Fig. 3b). Neat PEO and the PEO-20KETO mixture showed a decreasing complex viscosity
315 upon heating with a sharp decrease which indicated melting of the PEO crystals. KETO tended to
316 depress the melting point of PEO and reduced the complex viscosity of the drug-polymer mixture
317 compared to pure PEO. Schachter et al. showed that KETO/PEO interactions can be detected even in
318 non-melt processed blends at temperatures as low as 43 °C, hereby explaining the melting point
319 depression upon heating of the physical mixture (Schachter et al., 2004). Crystallization of the polymer
320 upon cooling from the melt occurred at lower temperatures for the PEO-20KETO mixture since
321 nucleation of polymer crystals is inhibited by KETO, confirming the previously described DSC
322 crystallization experiments. As for the PCL-20MPT mixture, the PCL crystals started melting at a
323 temperature of 56.8 °C during the first heating cycle. Moreover, MPT acted as a filler (i.e., increasing
324 the complex viscosity) above the melting point of PCL and below its own melting point (i.e., 123 °C),
325 but plasticized (i.e., lower complex viscosity) the molten mixture when the drug crystals melted.
326 Crystallization of PCL upon cooling is slightly inhibited by molten MPT since the crystallization
327 commenced at a lower temperature compared to pure PCL. During a second heating run of the PCL-
328 20MPT mixture, the viscosity decreased again to the same level as during the cooling run, indicating
329 only melting of the PCL crystals while MPT is dissolved in the matrix. Also, the melting point of PCL
330 during the second heating run was slightly lowered compared to the first heating cycle which can be
331 due to the refolding of the polymer chains into a less stable form compared to the original extended
332 chains. Based on the latter temperature sweep experiments, an extrusion temperature of 80 °C was
333 selected to process formulations while MPT maintained its crystalline state, while PCL/MPT mixtures
334 were extruded at 140 °C in order melt the drug fraction. Furthermore, based on the crystallization
335 kinetics during the temperature sweep test, 25 °C and 35 °C were chosen as mold temperatures to
336 produce the IM tablets. The lowest temperature (25 °C) was selected based on an anticipated fast
337 crystallization, while the highest temperature (35 °C) represented a temperature during which

338 crystallization was still ongoing during the temperature sweep experiment (showed in Fig. 3 by the
339 vertical dotted line), hence a slower crystallization is expected at this temperature.

340

341 3.1.3 Differential scanning calorimetry

342 The thermograms for physical mixtures containing PEO are shown in figure 4a. The first heating
343 cycle confirmed the previously described rheological temperature sweep results since the melting
344 point of PEO was depressed from 65.57 °C (pure PEO) to 63.54 °C (PEO-20KETO) and no melting
345 endotherm representing KETO crystals was observed, suggesting dissolution of KETO crystals in the
346 PEO matrix. The cooling cycle showed a higher crystallization temperature upon cooling of pure PEO
347 (40.92 °C) compared to the PEO-20KETO mixture (32.92 °C), confirming the previously described
348 crystallization inhibition theory. The thermograms of samples containing PCL are shown in figure 4b.
349 The first cycle showed melting of PCL and a second melting peak for MPT at 117 °C which is lower than
350 pure MPT (123 °C), suggesting partial dissolution of MPT crystals in the PCL matrix. Cooling of molten
351 MPT mixture showed a slightly lower polymer crystallization temperature (28.58 °C) as compared to
352 pure PCL (29.25 °C). On the other hand, when the PCL-20MPT mixture was only heated to 100 °C and
353 subsequently cooled, a higher crystallization temperature is measured (30.77 °C). This can be explained
354 by the nucleating effect of MPT crystals. The 40% MPT mixture showed the same trend as the
355 crystallization temperature was further increased to 31.33 °C.

356

357 3.2 Tablet characterization

358 3.2.1 Solid-state analysis and crystalline microstructure

359

360 The DSC results from the IM tablets are summarized in table 3. KETO was completely transformed
361 from the crystalline to the amorphous state during extrusion and subsequent injection molding. Also,
362 MPT was partially transformed to the amorphous state when extruded at 140 °C, but remained
363 crystalline when extruded at 80 °C. The crystallinity of PEO during annealing in the mold increased
364 significantly (from 66.29 to 70.14%) when annealed at 35 °C compared to annealing at 25 °C. On the
365 other hand, the PCL-20MPT and PCL-40MPT formulation processed at 80 °C and 140 °C did not show
366 a significant increase in the polymer crystallinity. However, the peak melting temperature did increase
367 (from 50.40 to 51.92 °C for PCL-20MPT; from 55.95 to 56.96 °C for PCL-40MPT), suggesting that the
368 polymer microstructure had changed. The reason for the polymer microstructural differences
369 originates from the various applied cooling rates. Higher cooling rates are obtained when cooling from
370 the melt to a lower mold temperature (25 °C), therefore giving less time to the melt to form more
371 perfect crystals due to the quick transition from a molten material to a structured crystalline solid
372 state. In order to confirm this hypothesis, the microstructure of the PCL crystals was visualized using
373 POM. The crystalline microstructure of pure PCL consists of impinged spherulite structures (Fig. 5).
374 Injection molding of pure PCL at 25 °C (Fig. 5a) gave smaller structures compared to the sample
375 collected after injection molding at 35 °C (Fig. 5b). A semi-quantitative analysis was performed and
376 provided as supplementary material (Fig SI2). Moreover, the incorporation of MPT crystals (Fig. 5 c-d)
377 in the melt reduced the size of the PCL microstructure at both injection mold temperatures (i.e., 25,
378 35 °C) compared to neat PCL.

379 3.2.2 Drug dissolution

380 *Immediate release formulation*

381 The cumulative release of KETO from the PEO matrix tablets is shown in figure 6. The release of
382 KETO from the IM tablets reached 100% within 4 hours. Calculated similarity ($f_2 = 70$) and difference
383 factor ($f_1 = 5$) indicated that there is no significant difference between the dissolution profiles of the
384 tablets injection molded at 25 °C and 35 °C. For immediate release formulations containing rapidly

385 erodible and water soluble semi-crystalline polymers, the drug dissolution is mainly controlled by
386 swelling and erosion of the polymer. For this low molecular weight PEO, erosion is the dominant
387 mechanism according to Cantin et al. (Cantin et al., 2016). Therefore, differences in polymer
388 crystallinity and microstructure are insignificant for controlling the drug dissolution for this type of
389 formulation. However, the drug release can be controlled by addition of erosion-promoting
390 substances. Crospovidone showed to increase the KETO release from PEO melt processed tablets by
391 increasing the rate of erosion of the PEO matrix (Schachter et al., 2004). Furthermore, the molecular
392 weight of PEO is well known to have an impact on the drug release (Cantin et al., 2016). High molecular
393 weight PEO is often used to provide sustained release of the API (Monteyne et al., 2016).

394 *Sustained release formulation*

395 The drug release profiles from the formulations containing 20% (w/w) MPT are shown in Fig.
396 7a. As a result of the poor wettability of the PCL matrix, a full release of the drug cannot be obtained
397 within 24 hours. The MPT release profile of the 20% MPT formulation showed a significant increase of
398 the total drug release when extruded above the drug melting point. This is due to MPT being partially
399 transformed to the amorphous state during extrusion (see table 3). However, no significant difference
400 in drug release was found between the tablets prepared at various mold temperatures (25 and 35 °C)
401 after extrusion at 140 °C. The variance of the drug release profile was higher for the tablets extruded
402 at 140 °C, which can be explained by the large variance in amorphous drug obtained (see table 3). On
403 the other hand, the drug release is significantly lower from tablets produced after extrusion at 80 °C
404 due to the crystalline state of the drug. Moreover, the drug release profiles from annealed tablets
405 molded at 25 °C and 35 °C were not significantly different according to the calculated similarity ($f_2 =$
406 61) and difference factor ($f_1 = 86$). However, the curves showed a certain similarity in shape but a more
407 pronounced burst-effect was observed for tablets prepared at mold temperature of 25 °C. It is well
408 known that polymer crystallinity and morphology has an impact on the water vapor permeability (Duan
409 and Thomas, 2014). Larger and more perfect crystals present a stronger barrier for water diffusion. By

410 increasing the drug load to 40% (w/w), a faster and more complete release of MPT was found (Fig. 7b).
411 Similar results are found for the 40% (w/w) MPT formulation wherein the tablets produced at 25 °C
412 showed a significant (factor $f_2 = 41$ and $f_1 = 84$) higher percentage drug release after 24 hours
413 compared to tablets prepared at a mold temperature of 35 °C. These differences in drug release
414 between both injection mold temperatures can be explained by the various crystal morphologies
415 obtained (shown in previous section). Larger and more perfect crystal lattices were obtained in case a
416 higher mold temperature was used. As a result, the drug diffusion rate through the water insoluble
417 matrix was decreased. Furthermore, the polymer microstructure of the tablets can change over time
418 during long term storage. Therefore, crystal growth and polymer degradation are likely to become
419 more important for the control of drug release at later time points.

420

421 4 **Conclusion**

422 The impact of the injection mold temperature upon the polymer crystallinity and microstructure
423 and hence the drug release was investigated. Isothermal crystallization experiments showed that the
424 temperature and the drug solid-state had an impact on the polymer crystallization kinetics. Molten or
425 dissolved drug inhibited the polymer crystallization, whereas a crystalline drug acted as
426 filler/nucleating agent, enhancing the polymer crystallization upon cooling from the melt. The polymer
427 crystallinity increased at higher mold temperatures for the PEO tablets but did not significantly change
428 for PCL tablets. The drug release from the PEO matrix was not affected by the various polymer
429 crystallinities induced by a difference in mold temperature. This is due to the erosion mechanism,
430 controlling the drug release for the immediate release formulation. On the other hand, the drug
431 release from the PCL matrix, which is purely diffusion controlled, was influenced by the polymer
432 microstructure. It is shown in this study that the polymer microstructure can be controlled by applying
433 various thermal histories. Larger polymer crystals are obtained using higher mold temperatures,
434 reducing the drug diffusion rate through the polymer matrix. These results imply that the injection

435 mold temperature should be carefully controlled for sustained release formulations containing
436 hydrophobic semi-crystalline polymers.

437 5 Acknowledgments

438 Perstorp is kindly acknowledged for providing CAPA™ 6506. Thermo Fisher is kindly acknowledged
439 for providing the injection molding system.

440

441 6 References

442 Alexis, F., 2005. Factors affecting the degradation and drug-release mechanism of poly(lactic acid) and
443 poly[(lactic acid)-co-(glycolic acid)]. *Polym. Int.* 54, 36–46. doi:10.1002/pi.1697

444 Bruce, L.D., Shah, N.H., Waseem Malick, A., Infeld, M.H., McGinity, J.W., 2005. Properties of hot-melt
445 extruded tablet formulations for the colonic delivery of 5-aminosalicylic acid. *Eur. J. Pharm.*
446 *Biopharm.* 59, 85–97. doi:10.1016/j.ejpb.2004.06.007

447 Cantin, O., Siepmann, F., Danede, F., Willart, J.F., Karrout, Y., Siepmann, J., 2016. PEO hot melt
448 extrudates for controlled drug delivery: Importance of the molecular weight. *J. Drug Deliv. Sci.*
449 *Technol.* 36, 130–140. doi:10.1016/j.jddst.2016.09.003

450 Clark, M.R., Johnson, T.J., McCabe, R.T., Clark, J.T., Tuitupou, A., Elgendy, H., Friend, D.R., Kiser, P.F.,
451 2012. A hot-melt extruded intravaginal ring for the sustained delivery of the antiretroviral
452 microbicide UC781. *J. Pharm. Sci.* 101, 576–587. doi:10.1002/jps.22781

453 Crist, B., Schultz, J.M., 2016. Polymer spherulites: A critical review. *Prog. Polym. Sci.* 56, 1–63.
454 doi:10.1016/j.progpolymsci.2015.11.006

455 Crowley, M.M., Fredersdorf, A., Schroeder, B., Kucera, S., Prodduturi, S., Repka, M. a, McGinity, J.W.,
456 2004. The influence of guaifenesin and ketoprofen on the properties of hot-melt extruded

457 polyethylene oxide films. *Eur. J. Pharm. Sci.* 22, 409–18. doi:10.1016/j.ejps.2004.04.005

458 Duan, Z., Thomas, N.L., 2014. Water vapour permeability of poly(lactic acid): Crystallinity and the
459 tortuous path model. *J. Appl. Phys.* 115. doi:10.1063/1.4865168

460 Fowler, J.N., Chapman, B.R., Green, D.L., 2010. Impact of plasticizers and tackifiers on the
461 crystallization of isotactic poly(1-butene). *Eur. Polym. J.* 46, 568–577.
462 doi:10.1016/j.eurpolymj.2009.11.013

463 Gupta, B., Geeta, Ray, A.R., 2012. Preparation of poly(ϵ -caprolactone)/poly(ϵ -caprolactone-co-
464 lactide) (PCL/PLCL) blend filament by melt spinning. *J. Appl. Polym. Sci.* 123, 1944–1950.
465 doi:10.1002/app.34728

466 Jeong, J.C., Lee, J., Cho, K., 2003. Effects of crystalline microstructure on drug release behavior of
467 poly(ϵ -caprolactone) microspheres. *J. Control. Release* 92, 249–258. doi:10.1016/S0168-
468 3659(03)00367-5

469 Kamaly, N., Yameen, B., Wu, J., Farokhzad, O.C., 2016. Degradable Controlled-Release Polymers and
470 Polymeric Nanoparticles: Mechanisms of Controlling Drug Release. *Chem. Rev.* 116, 2602–2663.
471 doi:10.1021/acs.chemrev.5b00346

472 Karavelidis, V., Karavas, E., Giliopoulos, D., Papadimitriou, S., Bikiaris, D., 2011. Evaluating the effects
473 of crystallinity in new biocompatible polyester nanocarriers on drug release behavior. *Int. J.*
474 *Nanomedicine* 6, 3021–3032. doi:10.2147/IJN.S26016

475 Lorenzo, A.T., Arnal, M.L., Albuerne, J., Müller, A.J., 2007. DSC isothermal polymer crystallization
476 kinetics measurements and the use of the Avrami equation to fit the data: Guidelines to avoid
477 common problems. *Polym. Test.* 26, 222–231. doi:10.1016/j.polymertesting.2006.10.005

478 Marentette, J.M., Brown, G.R., 1998. The crystallization of poly (ethylene oxide) in blends with neat

479 and plasticized poly (vinyl chloride). *Polymer (Guildf)*. 39, 1415–1427.

480 Monteyne, T., Adriaensens, P., Brouckaert, D., Remon, J.P., Vervaet, C., De Beer, T., 2016. Stearic acid
481 and high molecular weight PEO as matrix for the highly water soluble metoprolol tartrate in
482 continuous twin-screw melt granulation. *Int. J. Pharm.* 512, 158–167.
483 doi:10.1016/j.ijpharm.2016.07.035

484 Moore, J.W., Planner, H.H., 1996. Mathematical Comparison of Dissolution Profiles. *Pharm. Technol.*
485 20, 64–74.

486 Parikh, T., Gupta, S.S., Meena, A., Serajuddin, A.T.M., 2014. Investigation of thermal and viscoelastic
487 properties of polymers relevant to hot melt extrusion - III: Polymethacrylates and
488 polymethacrylic acid based polymers . *J. Excipients Food Chem* 5, 56–64.

489 Piorkowska, E., Galeski, A., Haudin, J.-M., 2006. Critical assessment of overall crystallization kinetics
490 theories and predictions. *Prog. Polym. Sci.* 31, 549–575. doi:10.1016/j.progpolymsci.2006.05.001

491 Prodduturi, S., Manek, R. V., Kolling, W.M., Stodghill, S.P., Repka, M.A., 2005. Solid-state stability and
492 characterization of hot-melt extruded poly(ethylene oxide) films. *J. Pharm. Sci.* 94, 2232–2245.
493 doi:10.1002/jps.20437

494 Rothen-Weinhold, A., Besseghir, K., Vuaridel, E., Sublet, E., Oudry, N., Kubel, F., Gurny, R., 1999.
495 Injection-molding versus extrusion as manufacturing technique for the preparation of
496 biodegradable implants. *Eur. J. Pharm. Biopharm.* 48, 113–121. doi:10.1016/S0939-
497 6411(99)00034-X

498 Schachter, D.M., Xiong, J., Tirol, G.C., 2004. Solid state NMR perspective of drug-polymer solid
499 solutions: A model system based on poly(ethylene oxide). *Int. J. Pharm.* 281, 89–101.
500 doi:10.1016/j.ijpharm.2004.05.024

501 Schick, C., 2009. Differential scanning calorimetry (DSC) of semicrystalline polymers. *Anal. Bioanal.*
502 *Chem.* 395, 1589. doi:10.1007/s00216-009-3169-y

503 Suwardie, H., Wang, P., Todd, D.B., Panchal, V., Yang, M., Gogos, C.G., 2011. Rheological study of the
504 mixture of acetaminophen and polyethylene oxide for hot-melt extrusion application. *Eur. J.*
505 *Pharm. Biopharm.* 78, 506–512. doi:10.1016/j.ejpb.2011.03.013

506 Sweetman, S. (Ed.), 2009. *Martindale: The Complete Drug Reference*, 36th Edition, 36 Slp Har. ed.
507 Pharmaceutical Press, London; Chicago.

508 Van Renterghem, J., Vervaet, C., De Beer, T., 2017. Rheological Characterization of Molten Polymer-
509 Drug Dispersions as a Predictive Tool for Pharmaceutical Hot-Melt Extrusion Processability.
510 *Pharm. Res.* doi:10.1007/s11095-017-2239-7

511 Verstraete, G., Van Renterghem, J., Van Bockstal, P.J., Kasmi, S., De Geest, B.G., De Beer, T., Remon,
512 J.P., Vervaet, C., 2016. Hydrophilic thermoplastic polyurethanes for the manufacturing of highly
513 dosed oral sustained release matrices via hot melt extrusion and injection molding. *Int. J. Pharm.*
514 506, 214–221. doi:10.1016/j.ijpharm.2016.04.057

515 Zhao, L., Kai, W., He, Y., Zhu, B., Inoue, Y., 2005. Effect of aging on fractional crystallization of
516 poly(ethylene oxide) component in poly(ethylene oxide)/poly(3-hydroxybutyrate) blends. *J.*
517 *Polym. Sci. Part B Polym. Phys.* 43, 2665–2676. doi:10.1002/polb.20552

518 Zilberman, M., 2005. Dexamethasone loaded bioresorbable films used in medical support devices:
519 Structure, degradation, crystallinity and drug release. *Acta Biomater.* 1, 615–624.
520 doi:10.1016/j.actbio.2005.06.007

521

522

523

Table 1: Isothermal crystallization experiments.

Samples	Melt equilibration temperature (°C)	Isothermal crystallization temperatures (°C)
PEO	100	46 – 47 – 48 – 49 – 50 – 51
PEO-20KETO	100	42 – 43 – 44 – 45 – 46 – 47
PCL	100	39 – 40 – 41 – 42 – 43 – 44
PCL-20MPT	80 and 140	39 – 40 – 41 – 42 – 43 – 44
PCL-40MPT	80	39 – 40 – 41 – 42 – 43 – 44

524

525

Table 2: Process parameters for HME and IM.

Formulation	Screw speed	Barrel temperature	Mold temperature	Solidification time
80 % PEO 20 % KETO	150 rpm	100 °C	25 °C	1 min
			35 °C	1 min
80 % PCL 20 % MPT	150 rpm	80 °C	25 °C	1 min
			35 °C	2 min
	150 rpm	140 °C	25 °C	2 min
			35 °C	3 min
60 % PCL 40 % MPT	150 rpm	80 °C	25 °C	1 min
			35 °C	1 min

529 Table 3: Polymer and drug crystallinity from IM tablets reported as average values with standard deviation between
 530 brackets (n = 6). E = extrusion barrel temperature; M = mold temperature. T_m = polymer peak melting point.

Sample	T _m (°C)	Polymer crystallinity (%)	Drug crystallinity (%)
80% PEO 20% KETO E = 100 °C M = 25 °C	55.45 (0.94)	66.29 (1.59)	Amorphous
80% PEO 20% KETO E = 100 °C M = 35 °C	56.08 (0.50)	70.14 (1.70)	Amorphous
80% PCL 20% MPT E = 80 °C M = 25 °C	55.99 (0.39)	50.40 (1.61)	95.48 (2.59)
80% PCL 20% MPT E = 80 °C M = 35 °C	56.75 (0.27)	51.92 (4.73)	96.96 (3.43)
80% PCL 20% MPT E = 140 °C M = 25 °C	56.58 (0.28)	52.63 (4.58)	20.98 (7.45)
80% PCL 20% MPT E = 140 °C M = 35 °C	56.99 (0.32)	52.72 (2.39)	13.11 (7.89)
60% PCL 40% MPT E = 80 °C M = 25 °C	55.95 (0.46)	48.57 (1.34)	98.65 (2.11)
60% PCL 40% MPT E = 80 °C M = 35 °C	56.96 (0.32)	50.85 (1.31)	99.67 (3.20)

531

532

533

534

535

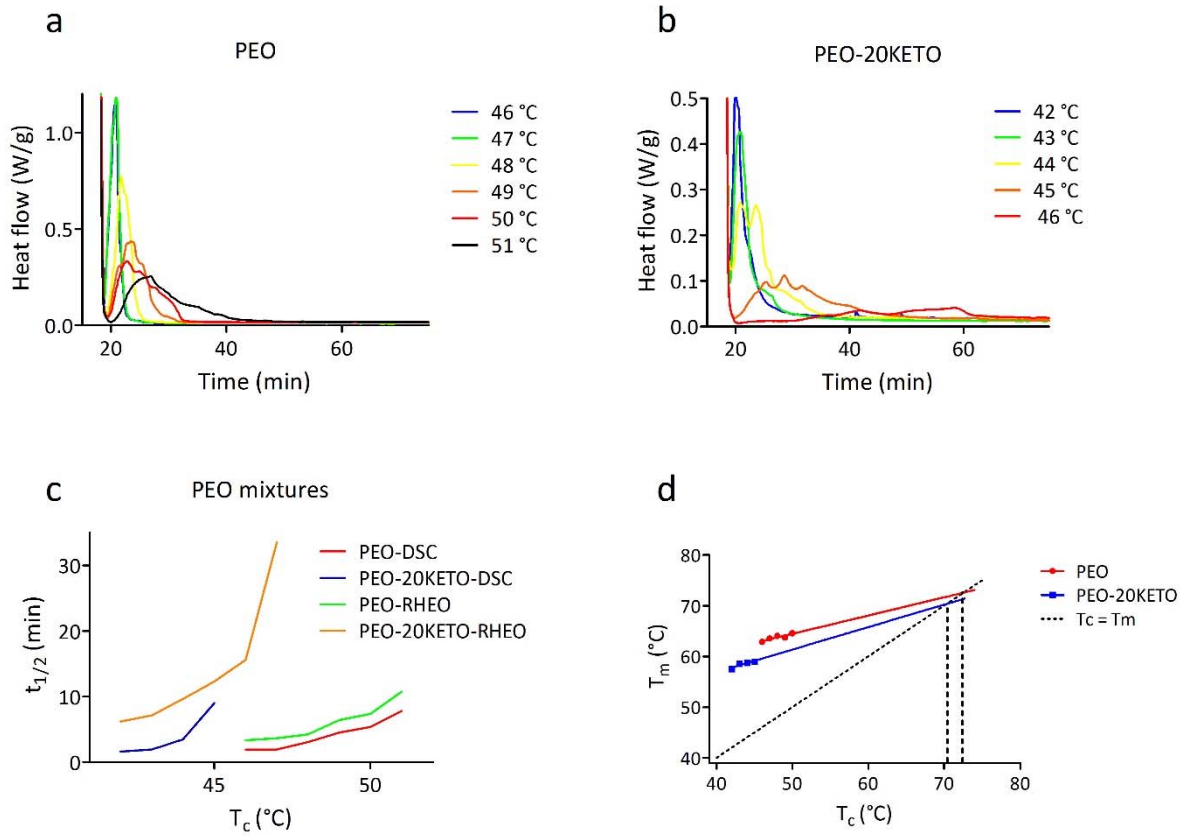
536

537

538

539

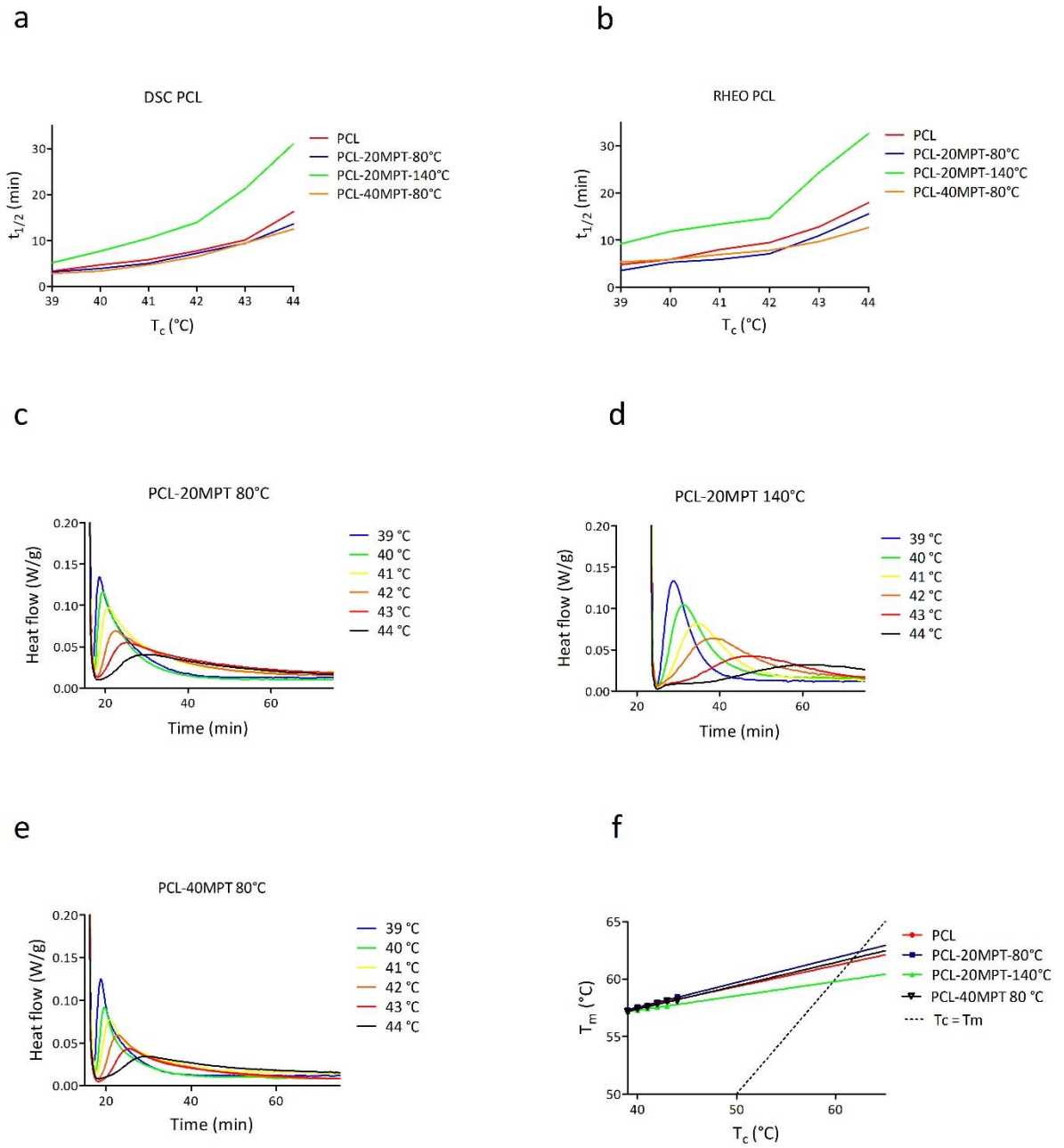
540



541

542 Figure 1: Heat flow during isothermal crystallization for (a) PEO and (b) PEO-20KETO. c) Half crystallization time vs
 543 isothermal crystallization temperature for PEO samples measured by DSC and Rheology. d) Hoffman-Weeks plot for samples
 544 containing PEO.

545



546

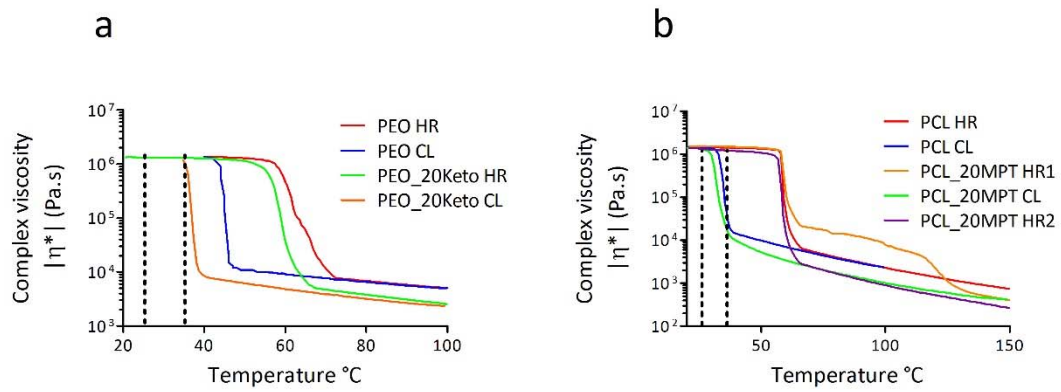
547 Figure 2: Half crystallization time as function of isothermal crystallization temperatures for samples containing PCL

548 measured by (a) DSC and (b) Rheology. Heat flow as function of isothermal time for PCL-20MPT below (c = 80 °C) and above

549 (d = 140 °C) drug melting point and PCL-40MPT (e) below the drug melting point. (f) Hoffman-Weeks plot for samples

550 containing PCL samples.

551

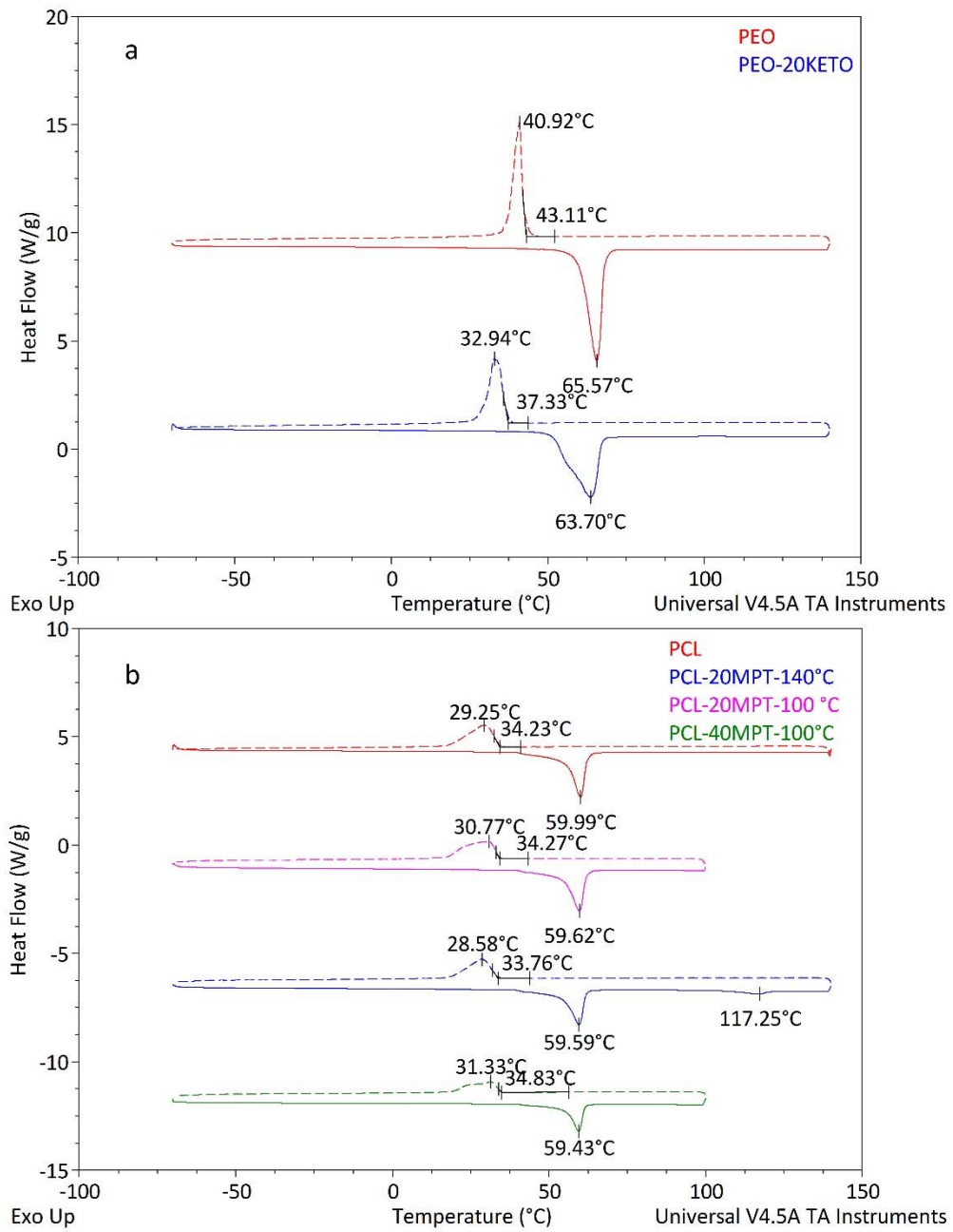


552

553 Figure 3: Rheological temperature sweep experiments for (a) PEO and PEO-20KETO and (b) PCL and PCL-20MPT. HR =

554 heating run, CL = Cooling run. Vertical dotted lines indicate 25 °C and 35 °C, which were chosen as mold temperatures.

555



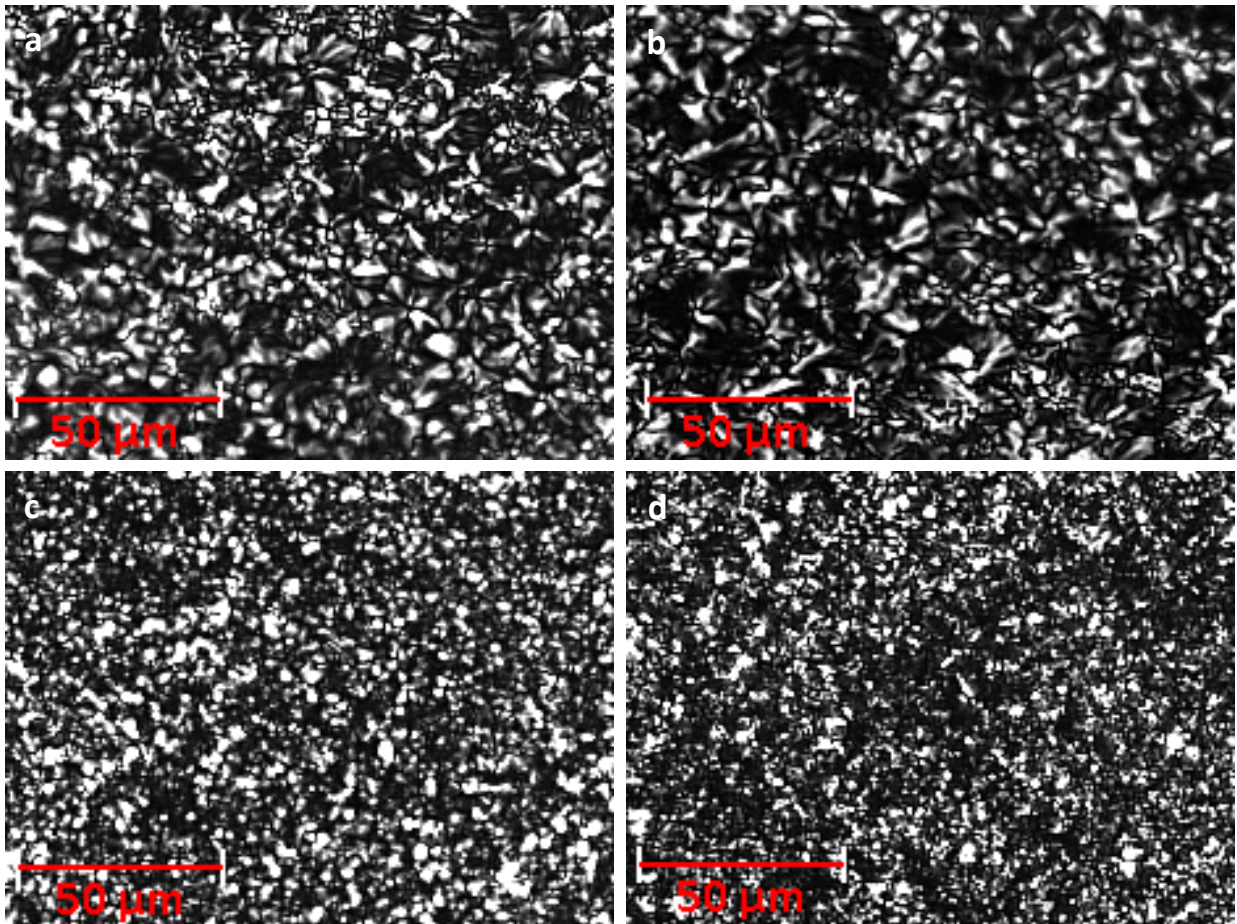
556

557 Figure 4: DSC thermograms of the first heating (solid line) and subsequent cooling phase (dashed line) of (a) PEO and PEO-

558 20KETO, and (b) PCL, PCL-20MPT and PCL-40MPT mixtures.

559

560

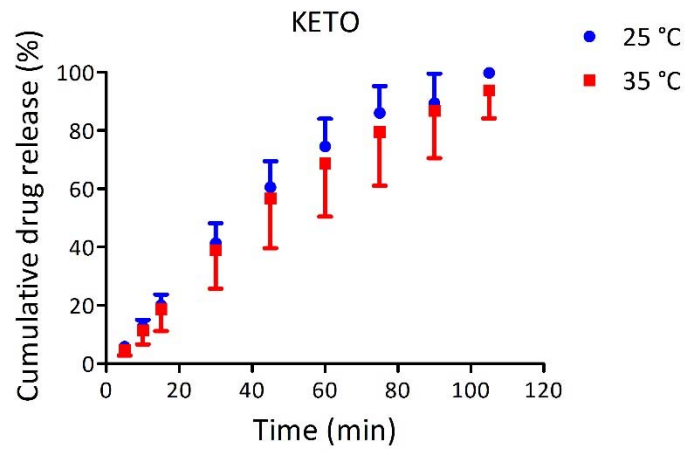


561

562 Figure 5: PCL extruded at 80 °C and injection molded at a) 25 °C and b) 35 °C. PCL-20MPT extruded at 80 °C and injection

563 molded at c) 25 °C and d) 35 °C. Magnification = 10 x

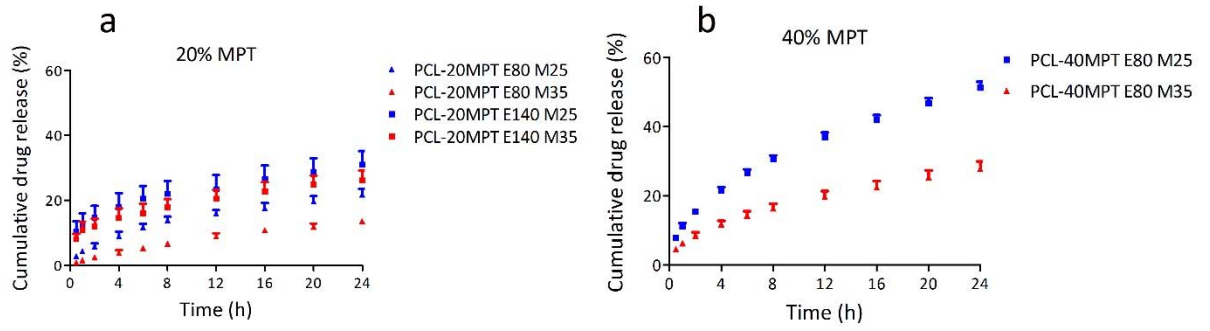
564



565

566 Figure 6: Cumulative drug release of PEO-20KETO formulation from tablets (n = 5) prepared at mold temperatures of 25
567 (blue dots) and 35 °C (red squares).

568



569

570 Figure 7: Cumulative drug release of (a) PCL-20MPT and (b) PCL-40MPT tablets (n = 5). E = extrusion temperature, M =
 571 mold temperature. The variance of the drug release is estimated by the standard deviation.

572

573

574

575

576

577

578

579

580

581

582

583

584

Supplementary information for

585 **The impact of the injection mold temperature upon polymer crystallization and resulting drug**
586 **release from immediate and sustained release tablets.**

587 Jeroen Van Renterghem*, Heleen Dhondt, Glenn Verstraete, Michiel De Bruyne, Chris Vervaet, Thomas
588 De Beer

589 *Corresponding author: Jeroen Van Renterghem

590 Laboratory of Process Analytical Technology, Ghent University, Ottergemsesteenweg 460, 9000 Ghent,
591 Belgium

592 TEL: 0032 9 264 8039

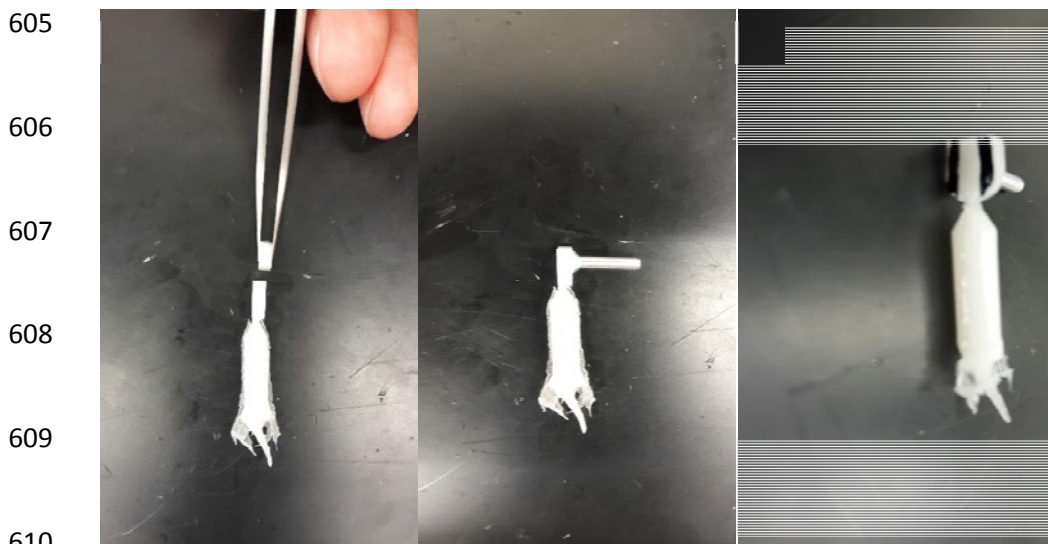
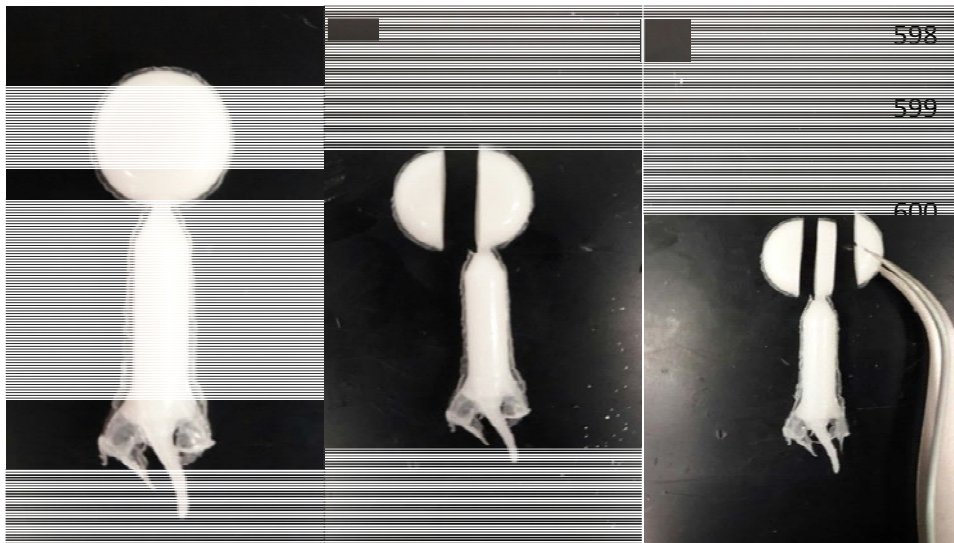
593 FAX: 0032 9 264

594 E-MAIL: jeroen.vanrenterghem@ugent.be

595

596

597 Trimming process.



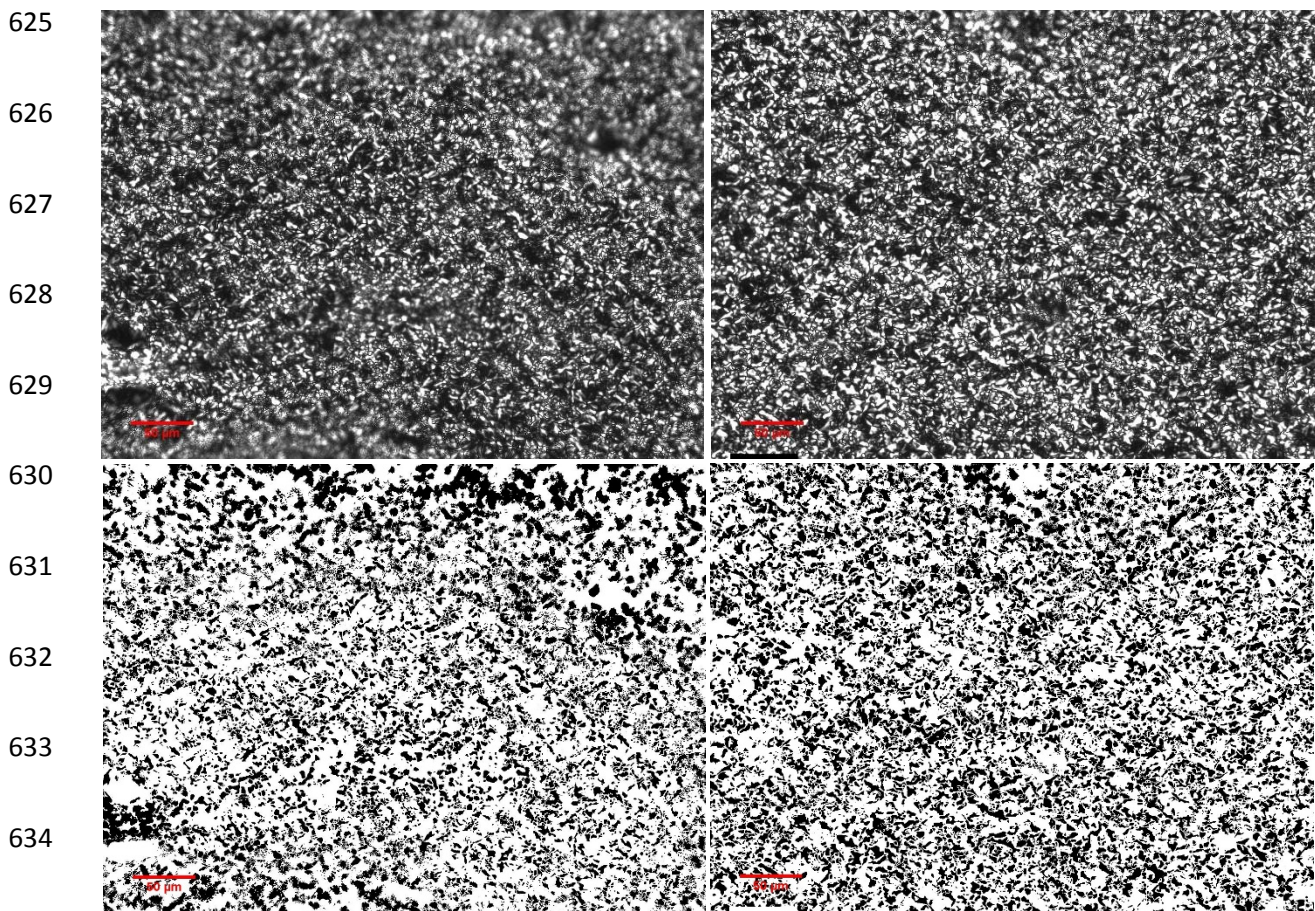
614 Figure S11: Trimming procedure to obtain samples before sectioning into thin (3 μ m) samples using a microtome. a) IM
615 tablet attached to the entry section (i.e., gate). b) Tablet cut in half with a razor blade. f) Trimming of the tablet and mounting
616 on an aluminum pin. g) Final sample obtained before cryosectioning.

617

618 Semi-quantitative analysis of POM images:

619 The background of the original images (Fig. SI2 a,b) was subtracted using the background treshold
620 option from imageJ. The remaining black structures of image c and d are related to the crystal
621 structures (i.e., spherulites). The structures of figure c (IM temperature: 25 °C) are smaller and of
622 greater number (5.57 μm , count: 8632) compared to the structures (7.77 μm , count: 7920) of figure d
623 (IM temperature: 35 °C).

624



636 Figure SI2: Original POM images of PCL extruded at 80 °C a) IM = 25 °C and b) IM = 35 °C. The same POM images after
637 subtraction of the background c) IM = 25 °C d) IM = 35 °C. Scale bar = 50 μm , magnification = 20x, IM = injection mold
638 temperature.

639

